

KG-QUEST: KNOWLEDGE GRAPH-ENHANCED QUESTION ANSWERING AND REASONING IN LARGE LANGUAGE MODELS

006 **Anonymous authors**

007 Paper under double-blind review

ABSTRACT

013 Large Language Models (LLMs) achieve strong results on medical and open-
 014 domain QA but remain limited by static retrieval and parametric memory, hin-
 015 dering adaptation to evolving ontologies and multi-hop reasoning. We present
 016 KG-QUEST, a framework for Knowledge Graph-Enhanced QA that grounds ques-
 017 tions in Entity-Attribute-Value (EAV) and Entity-Relation-Entity (ERE) triples
 018 and dynamically discovers an answer-specific knowledge graph during inference.
 019 A query graph is softly matched to a global biomedical KG and expanded via
 020 hop-limited frontier search with predicate weights, synonym/inverse alignment,
 021 and negation-aware pruning to form a minimal, high-support subgraph. Phase I
 022 (KG generation) fine-tunes LLaMA 3.1 (8B) with ensemble refinement to produce
 023 ontology-aligned triples; answers are then selected by dual grounding—scoring KG
 024 paths (and optional text evidence) with hop decay and abstention—yielding explicit
 025 evidence chains. On *MedQA (USMLE)* and *MMLU medical subsets*, KG-QUEST
 026 establishes new state-of-the-art results (93.7% and 92.0% accuracy, respectively),
 027 surpassing GPT-4 and Med-PaLM 2 while maintaining verifiability. Beyond medi-
 028 cal QA, KG-QUEST shows how LLMs can not only retrieve but also construct and
 029 navigate structured knowledge graphs for complex reasoning.

1 INTRODUCTION

030 Large Language Models (LLMs) have achieved strong results on open-domain and medical QA,
 031 yet they remain constrained by static parametric memory and brittle retrieval-augmented generation
 032 (RAG) pipelines. In high-stakes healthcare settings, precise alignment with evolving ontologies
 033 (e.g., FHIR, UMLS, SNOMED) and sensitivity to patient context are essential; current systems
 034 still suffer from hallucinations, stale knowledge, and limited ability to *adapt representations during*
 035 *inference*. Hybrid KG-text approaches such as GraphRAG (Edge et al., 2024), Chain-of-Knowledge
 036 (Li et al., 2024), and ToG-2 (Ma et al., 2025) highlight the promise of coupling retrieval with
 037 knowledge graphs (KGs), but often rely on prompt heuristics, Wiki-centric coverage, or fragile entity
 038 linking. In healthcare-specific pipelines, KARE (Jiang et al., 2025) shows that EHR-anchored KG
 039 construction with community retrieval improves clinical prediction on MIMIC (Johnson et al., 2016;
 040 2023), while KG-SFT (Chen et al., 2025) boosts multilingual medical QA by injecting KG-grounded
 041 explanations into supervised fine-tuning—at the cost of curated resources and training overhead.
 042 Meanwhile, interactive benchmarks like AGENTCLINIC (Schmidgall et al., 2024) move beyond
 043 static exam-style QA (Jin et al., 2019; 2021; Singhal et al., 2023a; Hendrycks et al., 2020) toward
 044 sequential, multimodal, and bias-sensitive evaluation, underscoring the need for *dynamic* reasoning
 045 under incomplete information.

046 We introduce *KG-QUEST* (*Knowledge Graph-Enhanced Question Answering and Reasoning in*
 047 *LLMs*), a framework that integrates LLMs with an *answer-specific, dynamically discovered knowledge*
 048 *graph* built on-the-fly from the question. The key idea is to represent questions with *Entity-Attribute-*
 049 *Value (EAV)* and *Entity-Relation-Entity (ERE)* triples, aligning natural language to ontology-grounded
 050 structure. From these triples we construct a *query graph* that is softly matched to a global biomedical
 051 KG; we then perform hop-limited frontier expansion with predicate-specific weights, synonym/inverse
 052 handling, and negation-aware pruning to discover the minimal, high-support subgraph sufficient
 053 to answer the question. This subgraph is scored with *dual grounding* (KG paths + optional text

054 evidence), uncertainty-aware hop decay, and an abstention rule, producing answers accompanied by
 055 explicit evidence chains.
 056

057 *Phase I (KG generation) uses a fine-tuned LLaMA 3.1 (8B) model* as the triple extractor. We fine-tune
 058 it to produce ontology-aligned EAV/ERE triples, canonical entity mentions (synonyms/inverses), and
 059 negation-aware predicates. Multiple extraction variants are combined via ensemble refinement to
 060 obtain calibrated reliabilities, which seed the dynamic discovery process.
 061

062 Concretely, KG-QUEST comprises: (i) an *ensemble-refined seed* produced by the fine-tuned
 063 LLaMA 3.1 (8B) extractor and a triple-scoring model to yield calibrated EAV/ERE edges aligned
 064 to the ontology; (ii) a *query-graph-guided dynamic discovery* stage that matches nodes/relations,
 065 expands neighborhoods with hop decay and boundary detection, and constructs a compact answer-
 066 specific KG; and (iii) an *answer selection* module that aggregates path evidence with dual (KG+text)
 067 grounding and returns both the choice and a verbalized justification. This design departs from static
 068 clustering and prompt-only reasoning: the *question itself* becomes a structural constraint that shapes
 069 the evidence graph used for answering.
 070

071 **Contributions.** (1) A *query-graph-guided dynamic KG* procedure that discovers, scores, and
 072 *bounds* an answer-specific subgraph via hop-limited frontier expansion, predicate weighting, syn-
 073 onym/inverse alignment, and negation-aware pruning. (2) A *dual-grounded scoring* objective that
 074 composes ER-weighted EAV/ERE paths and optionally fuses textual evidence, with uncertainty-aware
 075 hop decay and abstention for safety. (3) *Empirical gains* on standard QA benchmarks (e.g., *MedQA*,
 076 *PubMedQA*, *MMLU*) (Jin et al., 2021; 2019; Hendrycks et al., 2020), with transparent evidence chains
 077 and improved robustness under incomplete graphs and noisy linking.
 078

079 By unifying ontology-grounded representation with *dynamic KG* discovery and dual grounding—and
 080 by fine-tuning LLaMA 3.1 (8B) explicitly for Phase I KG generation—KG-QUEST advances a
 081 paradigm in which LLMs not only retrieve facts but also *construct and navigate* the structured
 082 knowledge needed for clinically meaningful reasoning.
 083

084 2 RELATED WORK

085 **Static KGE vs. LLM-driven KG discovery.** Classical KGE models—TransE, DistMult, ComplEx,
 086 RotatE—learn fixed embeddings and triple scorers on a *static*, closed-world schema Bordes et al.
 087 (2013); Yang et al. (2014); Trouillon et al. (2016); Sun et al. (2019). They capture algebraic relation
 088 patterns efficiently, but struggle with *open-world* additions (unseen entities/relations) and offer
 089 limited evidence traceability. In contrast, LLM-driven extraction discovers *new* EAV/ERE facts
 090 from unstructured corpora and aligns them to ontologies, enabling schema-flexible KG growth with
 091 natural-language rationales Pan et al. (2024); Chen et al. (2025). *KG-QUEST* bridges these lines by
 092 combining ontology-aligned triples with *query-graph-guided*, *dynamic* graph discovery that operates
 093 in an open-world setting while preserving verifiable evidence paths.
 094

095 **LLMs for medical QA.** Foundation LLMs (e.g., GPT-4, PaLM/Flan-PaLM) achieve strong results
 096 on MedQA/PubMedQA, especially with instruction tuning and safety-aware decoding Chowdhery
 097 et al. (2023); Achiam et al. (2023). Med-PaLM and Med-PaLM 2 further improve reasoning via
 098 ensemble refinement and chain-of-retrieval (CoR) Singhal et al. (2023b; 2025). *KG-QUEST* is
 099 complementary: instead of relying solely on generator-side advances, it *structures the reasoning*
 100 *substrate* as an answer-specific KG discovered from the question, enabling explicit multi-hop paths,
 101 uncertainty handling (hop decay, negation), and abstention.
 102

103 **Hybrid KG-text retrieval.** Graph-augmented RAG links corpus elements into graphs for multi-
 104 hop reasoning (e.g., GraphRAG, Chain-of-Knowledge, ToG-2) Edge et al. (2024); Li et al. (2024);
 105 Ma et al. (2025), and Self-RAG learns *when* to retrieve Asai et al. (2024). These systems interleave
 106 retrieval with graph exploration but often lack a tight mechanism to *constrain* graph growth to
 107 the question. *KG-QUEST* performs *query-graph matching with hop-limited frontier expansion*
 108 and explicit *boundary discovery* of a minimal, answer-sufficient subgraph, then scores it with dual
 109 grounding (KG+text), improving precision under noisy linking and incomplete KGs.
 110

108 **Healthcare KGs for reasoning.** Clinical systems such as KARE assemble UMLS- and PubMed-
 109 based subgraphs and score patient-centric communities Jiang et al. (2025); Bodenreider (2004);
 110 Canese & Weis (2013); Johnson et al. (2016; 2023). While effective, they rely on curated resources
 111 and largely *static* communities. *KG-QUEST* instead builds a *question-specific* dynamic KG via query
 112 alignment and neighborhood discovery, emphasizing just-enough structure for the current question
 113 and producing auditable evidence chains.

114 **KG-enhanced fine-tuning.** KG-SFT augments supervised fine-tuning data with KG-grounded
 115 explanations, improving multilingual medical QA Chen et al. (2025). Unlike this *training-time*
 116 augmentation, *KG-QUEST* focuses on *inference-time* dynamic KG construction and scoring, reducing
 117 dependence on curated expansions while retaining verifiability and controllable uncertainty.

118 **Positioning.** In summary, *KG-QUEST* unifies ontology-grounded EAV/ERE representation with
 119 *query-guided*, *dynamic* KG discovery and dual grounding. This departs from static KGE and
 120 complements retrieval-augmented LLMs by using the *question as a structural constraint* that shapes
 121 the evidence graph, yielding precise multi-hop reasoning with explicit uncertainty and abstention.

124 3 METHOD

125 We introduce *KG-QUEST*, a framework for medical QA that extends retrieval-augmented generation
 126 (RAG) with structured reasoning over *Entity–Attribute–Value (EAV)* and *Entity–Relation–Entity (ERE)*
 127 triples. *KG-QUEST* integrates LLMs with an *answer-specific, dynamically discovered knowledge*
 128 *graph*, built on-the-fly by matching a query graph to a global biomedical KG and expanding through
 129 scored neighborhoods. Unlike prior pipelines relying on static clustering or fixed retrieval, *KG-QUEST*
 130 explicitly *discovers the boundary* of a minimal, high-support subgraph sufficient to answer
 131 the question. The framework is formalized in Algorithm 1.

134 3.1 REPRESENTING QUESTIONS AS EAV/ERE TRIPLES AND A QUERY GRAPH

135 Each natural-language question q is mapped to triples

$$137 \quad q \mapsto \mathcal{T}(q) = \{t_i\}_{i=1}^N, \quad t_i \in \{\langle e, a, v \rangle, \langle e, r, e' \rangle\}. \quad (1)$$

138 *EAV* encodes descriptive properties (e.g., *Patient–Symptom–Chest pain*); *ERE* captures relational
 139 links (e.g., *Chest pain–indicates–MI*). We then form a *query graph* $\mathcal{Q} = (\mathcal{V}_q, \mathcal{R}_q, \mathcal{E}_q)$ by wiring
 140 the triples from $\mathcal{T}(q)$; nodes/edges inherit lexical labels, ontology hints, and type constraints (e.g.,
 141 UMLS/SNOMED).

143 3.2 PHASE I: SEED GRAPH VIA ENSEMBLE REFINEMENT (ER)

144 We obtain m diverse triple sets $\{\mathcal{T}^{(j)}\}_{j=1}^m$ using prompt/seed/tool variants, aggregate to $\mathcal{T}_{\text{pool}}$, and
 145 estimate a calibrated consensus score $\tilde{s}_{\text{ER}}(t)$ for each triple. Entities/relations are aligned to ontology
 146 concepts, yielding a seed subgraph

$$147 \quad \mathcal{G}_0 = \text{KGG}(\mathcal{T}_{\text{pool}}) \cup \text{OntologyAlign}(\mathcal{T}_{\text{pool}}, \mathcal{O}). \quad (2)$$

148 A triple-scoring model f_θ provides $s_{\text{KG}}(t)$; we fuse with ER via $s^*(t) = \lambda \tilde{s}_{\text{ER}}(t) + (1 - \lambda) s_{\text{KG}}(t)$
 149 and prune under threshold τ to obtain \mathcal{G}_1 .

152 3.3 PHASE II: DYNAMIC KG DISCOVERY VIA QUERY-GRAPH MATCHING

153 **Node/edge matching.** We create soft alignments from \mathcal{Q} to the global KG $\mathcal{G} = (\mathcal{V}, \mathcal{R}, \mathcal{E})$:

$$154 \quad \phi(v_q) \in \mathcal{V}, \quad \psi(r_q) \in \mathcal{R},$$

155 selected by a match score

$$156 \quad M(v_q \rightarrow u) = \underbrace{\text{lex}(v_q, u)}_{\text{string/synonym}} + \underbrace{\text{sem}(v_q, u)}_{\text{type/embedding}} + \underbrace{\text{ont}(v_q, u)}_{\text{ontology prior}},$$

157 and analogously for $M(r_q \rightarrow r)$, with inverse-relations allowed. Synonym expansion Σ (e.g., *palatine*
 158 *process* \leftrightarrow *palatine shelf*) prevents surface-form mismatch.

162 **Query-guided frontier expansion.** Starting from the matched anchors $\Phi_0 = \{\phi(v_q)\}$, we maintain
 163 a frontier \mathcal{F}_t and a discovered subgraph \mathcal{G}_t (initialized with \mathcal{G}_1 and anchor nodes). At step t we pop
 164 the highest-priority frontier node u and expand to neighbors $u' \in \mathcal{N}(u)$ if they improve alignment to
 165 some pending query edge $(v_q \xrightarrow{r_q} v'_q) \in \mathcal{E}_q$. Each candidate edge $(u \xrightarrow{r} u')$ receives
 166

$$\text{EdgeScore} = w(r) \cdot \alpha^{h(u)} \cdot M(v_q \rightarrow u) \cdot M(r_q \rightarrow r) \cdot M(v'_q \rightarrow u') \cdot \mathbb{I}_{\text{no-neg}}, \quad (3)$$

167 where $h(u)$ is hop distance from anchors, $w(r)$ encodes predicate specificity (`causes`
 168 `associated_with` `> found_in`), $\alpha \in (0, 1]$ applies hop decay, and $\mathbb{I}_{\text{no-neg}}$ nulls edges hitting
 169 negated predicates (e.g., `not_fusion_time`). Approved edges/nodes are added to \mathcal{G}_t and new
 170 neighbors join the priority queue.
 171

173 **Boundary discovery and stopping.** We define the boundary $\partial\mathcal{G}_t$ as active frontier nodes. Expansion
 174 stops when any of the following holds:
 175

$$(i) \Delta U_t < \varepsilon, \quad (ii) \text{max-hop} \geq H_{\max}, \quad (iii) \text{all query edges are matched above } \tau_m, \quad (4)$$

176 where ΔU_t is marginal utility (increase in total matched-query support), $H_{\max} \leq 3$, and τ_m is a match
 177 threshold. The result is a compact, answer-specific dynamic graph $\widehat{\mathcal{G}} = \mathcal{G}_t$ and a mapping between \mathcal{Q}
 178 and $\widehat{\mathcal{G}}$.
 179

181 **Optional retrieval check.** When the KG lacks direct support, we issue structured lookups from
 182 missing query edges to a corpus and extract candidate triples for verification. Retrieved triples are
 183 fused using a combined score:
 184

$$\text{TotalScore} = \lambda_{\text{kg}} \cdot \text{EdgeScore} + \lambda_{\text{text}} \cdot s_{\text{text}}, \quad (5)$$

186 where s_{text} is the textual retrieval score and $\lambda_{\text{kg}}, \lambda_{\text{text}}$ balance KG-based and text-based evidence. A
 187 small retrieval budget ensures efficiency.
 188

189 3.4 PHASE III: ANSWER SELECTION OVER THE DISCOVERED DYNAMIC KG

191 Let $\mathcal{O} = \{o_1, \dots, o_4\}$ be the answer options. For each o_k , we treat its node(s) (plus synonyms) as
 192 targets in $\widehat{\mathcal{G}}$ and score all paths connecting anchors to o_k . For a path $P = (v_0 \xrightarrow{r_1} \dots \xrightarrow{r_L} v_L)$ inside
 193 $\widehat{\mathcal{G}}$,

$$\text{score}(P) = \left(\prod_{i=1}^L w(r_i) \right) \cdot \alpha^L \cdot \text{sim}(q, P) \cdot \mathbb{I}_{\text{no-neg}}(P), \quad (6)$$

197 and the option score is $S(o_k) = \sum_{P \in \mathcal{P}(o_k)} \text{score}(P)$. We add a small clinical-context term $R_{\text{ctx}}(o_k)$
 198 (templates for ethics/statistics/trial design) and compute

$$S_{\text{total}}(o_k) = \lambda S(o_k) + (1 - \lambda) R_{\text{ctx}}(o_k), \quad \hat{o} = \arg \max_{o_k} S_{\text{total}}(o_k), \quad (7)$$

201 with abstention if $\max_k S_{\text{total}}(o_k) < \tau$. KG-QUEST returns \hat{o} and a verbalized justification from the
 202 highest-scoring path(s).
 203

204 **Why dynamic discovery?** Replacing static clustering with query-graph-guided expansion (i)
 205 concentrates computation on question-relevant neighborhoods, (ii) discovers just-enough structure to
 206 satisfy all query edges, and (iii) produces a smaller, auditable subgraph that transfers better across
 207 unseen layouts.
 208

209 3.5 END-TO-END LOOP

$$q \Rightarrow \mathcal{T}_{\text{pool}} \Rightarrow \mathcal{G}_0 \Rightarrow \mathcal{G}_1 \Rightarrow \text{Query-Graph Matching} \Rightarrow \widehat{\mathcal{G}} \Rightarrow \hat{o}. \quad (8)$$

211 **Complexity.** If b is the average branching factor and $H_{\max} \leq 3$, expansion is $O(b^{H_{\max}})$ per anchor
 212 (small in medical KGs). Scoring is linear in retrieved paths. Synonym expansion and negation
 213 pruning reduce the effective frontier.
 214

216 **Algorithm 1** KG-QUEST with Query-Graph Matching and Dynamic Boundary Discovery
217
218 **Require:** Question q , LLM \mathcal{L} , ontology \mathcal{O} , global KG \mathcal{G} , triple scorer f_θ , hop decay α , thresholds
219 (τ, τ_m) , budgets (H_{\max}, B)
220 **Ensure:** Answer \hat{o} , discovered dynamic KG $\hat{\mathcal{G}}$, evidence \mathcal{E}
221 1: *Phase I: ER seed.* Extract $\{\mathcal{T}^{(j)}\}$; aggregate $\mathcal{T}_{\text{pool}}$ with \tilde{s}_{ER} . Build \mathcal{G}_0 , fuse with s_{KG} to get \mathcal{G}_1 .
222 2: Build query graph \mathcal{Q} from $\mathcal{T}(q)$ with synonym set Σ and predicate map $\mathcal{M}_{\text{pred}}$.
223 3: *Phase II: Dynamic discovery.*
224 4: Compute anchor matches Φ_0 and initialize frontier \mathcal{F}_0 ; set $\mathcal{G}_0 \subseteq \mathcal{G}_1$ as seed of \mathcal{G}_t .
225 5: **while** stopping criteria not met **do**
226 6: Pop $u \in \mathcal{F}_t$; for neighbors $u' \in \mathcal{N}(u)$ compute Eq. (3); add approved edges to \mathcal{G}_t ; push new
227 frontier nodes.
228 7: Optionally retrieve & verify missing query edges with budget B ; integrate verified triples.
229 8: **end while**
230 9: $\hat{\mathcal{G}} \leftarrow \mathcal{G}_t$.
231 10: *Phase III: Answering.* Score options via Eqs. (6)–(7); return \hat{o} and justification.

4 REPRESENTATION LEARNING

At the core of *KG-QUEST* is a multi-view learner that jointly embeds: (i) ontology-aligned EAV/ERE triples, (ii) question semantics, and (iii) evidence signals from *dual grounding* (KG structure + text). Unlike static pipelines, representation learning in KG-QUEST is tightly coupled to the *dynamic knowledge-graph discovery* process in Sec. 3.3: a query graph derived from the question guides node/edge matching, hop-limited neighborhood expansion, and boundary detection of an *answer-specific* subgraph. We detail (a) ER-weighted triple embeddings; (b) path composition and question alignment with dual grounding on the discovered subgraph; and (c) how *query-graph matching + boundary discovery* act as representation-learning operators that replace static clustering.

4.1 EMBEDDING EAV/ERE TRIPLES WITH ENSEMBLE REFINEMENT

Given m extraction variants, we pool triples $\mathcal{T}_{\text{pool}} = \bigcup_{j=1}^m \mathcal{T}^{(j)}$, compute an ensemble-refined consensus $\tilde{s}_{\text{ER}}(t) \in [0, 1]$ (majority/Borda/learned combiner), and a KG model score $s_{\text{KG}}(t) = f_\theta(h, r, u)$. We then define a calibrated reliability

$$w(t) = \sigma(\lambda \tilde{s}_{\text{ER}}(t) + (1 - \lambda) s_{\text{KG}}(t)), \quad \lambda \in [0, 1],$$

with σ logistic.

For **EAV** triples $t = \langle e, a, v \rangle$ and **ERE** triples $t = \langle e, r, e' \rangle$, we embed and calibrate as

$$t_{\text{EAV}} = f_\phi([e; a; v]), \quad t_{\text{ERE}} = g_\phi(e, r, e'), \quad \tilde{t} = w(t) \cdot t,$$

where \tilde{t} (ER-calibrated) serves as the primitive for path and subgraph composition.

4.2 QUESTION-GRAPH ALIGNMENT OVER THE DISCOVERED DYNAMIC KG

Let $\hat{\mathcal{G}}$ denote the *dynamic* subgraph produced by query-graph matching and frontier expansion (Sec. 3.3). We encode the question q as $q \in \mathbb{R}^d$. Consider a path $p = (t_1, \dots, t_L)$ in $\hat{\mathcal{G}}$ with ER-calibrated triples $\{\tilde{t}_\ell\}$. We compose a question-aware path embedding with attention that also injects *query-match priors* from the discovery stage:

$$\alpha_\ell \propto \underbrace{w(t_\ell)}_{\text{ER reliability}} \underbrace{m(t_\ell)}_{\text{query-match prior}} \exp(\eta \cos(q, \tilde{t}_\ell)), \quad p = \sum_{\ell=1}^L \alpha_\ell \tilde{t}_\ell. \quad (9)$$

Here $m(t)$ summarizes the structural priors used during expansion:

$$m(t) = w(r) \cdot \alpha^{\text{hop}(t)} \cdot \underbrace{M_{\text{node}}(t) M_{\text{edge}}(t)}_{\text{query-graph alignment}},$$

where $w(r)$ is a predicate specificity weight (`causes`> `associated_with` > `found_in`), $\alpha \in (0, 1]$ is hop decay, and $M_{\text{node}}, M_{\text{edge}}$ are the soft node/edge match scores from Sec. 3.3.

270 **Dual grounding (KG + text).** If optional text evidence $\mathcal{E}(p)$ was fetched for missing query edges,
 271 we encode it as $e(p)$ and score
 272

$$273 \quad G(q, p) = g_{\text{KG}}(q, p) + \beta g_{\text{text}}(q, e(p)) - \gamma u(p), \quad (10)$$

274 where $u(p)$ is an uncertainty penalty (e.g., attention entropy or ER variance), $\beta, \gamma \geq 0$. Answer
 275 selection in Phase III maximizes a sum of such path scores that reach each option.
 276

277 **Training objectives (optional).** With supervision (gold path p^+ or answer links),
 278

$$279 \quad \mathcal{L}_{\text{InfoNCE}} = -\log \frac{\exp(G(q, p^+))}{\exp(G(q, p^+)) + \sum_{p^- \in \mathcal{N}} \exp(G(q, p^-))}, \quad (11)$$

$$282 \quad \mathcal{L}_{\text{cons}} = \sum_{t \in p^+} \max(0, \tau - s_{\text{KG}}(t)) + \text{CE-Calib}(\tilde{s}_{\text{ER}}), \quad (12)$$

284 encouraging dual-grounded alignment and calibrated confidence.
 285

286 4.3 QUERY-GRAPH MATCHING, BOUNDARY DISCOVERY, AND ITERATIVE REFINEMENT

288 KG-QUEST performs *dynamic representation learning* without static clustering by (i) *query-graph*
 289 *matching*, which restricts candidate nodes/edges to those satisfying the typed constraints of the
 290 question, concentrating attention mass and reducing negative sampling variance; (ii) *frontier expansion*
 291 with *hop decay*, which regularizes path length and predicate specificity via $m(t)$; and (iii) *boundary*
 292 *discovery*, which halts expansion when marginal utility falls below a threshold, yielding a compact,
 293 answer-specific subgraph $\hat{\mathcal{G}}$ that serves as an inductive bias for Eq. 9–10. Empirically, this improves
 294 sample efficiency and stabilizes learning relative to global, static neighborhoods.

295 At iteration t , KG-QUEST selects the best path $p^* = \arg \max_{p \subset \hat{\mathcal{G}}} G(q, p)$, identifies unmatched
 296 query edges along p^* , and (if needed) retrieves verifiable text to propose $\Delta\mathcal{T}$. New triples are
 297 ER-scored and integrated; embeddings are updated by weighting each triple with its reliability score
 298 and composing

$$299 \quad p_{t+1} \leftarrow \text{Compose}(\{\tilde{t}\} \cup \Delta\tilde{t}; q),$$

301 reducing uncertainty $u(p)$ until convergence or budget exhaustion. In effect, frontier operations
 302 (match → expand → stop) become feature operations (filter → weight → compose).

303 The procedure admits a constrained EM view: the *E-step* (evidence) comprises query-graph matching,
 304 frontier expansion, and optional retrieval that propose structure and assign priors $m(t)$; the *M-step*
 305 (model) fuses ER/KG reliability scores with dual-grounded scoring (Eq. 10) to re-weight and compose
 306 representations for maximum alignment. Thus, KG-QUEST functions as a dynamic, dual-grounded
 307 representation learner whose hypothesis space is carved by the question itself, not by static clustering
 308 of a global graph.

310 5 EXPERIMENTAL RESULTS

312 5.1 DATASETS

314 We evaluate on two complementary benchmarks that together cover clinical reasoning and broad
 315 general knowledge. Table 1 compares *MedQA* (*USMLE*) Jin et al. (2020) and *MMLU* Hendrycks et al.
 316 (2021). *MedQA* emphasizes clinical reasoning via vignette-style multiple-choice questions (MCQs),
 317 whereas *MMLU* spans 57 subjects (STEM, humanities, and social sciences) with standardized
 318 4-option MCQs. Both report top-1 accuracy (*MMLU* often under few-shot prompts).

319 Beyond the aggregate *MMLU* score, we also evaluate on six *MMLU* *medical subsets* to obtain
 320 fine-grained medical performance. Table 2 lists the datasets used in our experiments: the *core*
 321 benchmark (*MedQA*) and the *MMLU* medical subsets (Clinical Knowledge, Medical Genetics,
 322 Anatomy, Professional Medicine, College Biology, College Medicine), with sizes ranging from 100
 323 to 272 items. This configuration provides a balanced mix of large-scale clinical evaluation (*MedQA*,
 1,273 items) and targeted medical domains (e.g., Medical Genetics, 100 items).

Table 1: Comparison of two QA datasets used in biomedical and general-domain evaluation.

Property	MedQA (USMLE) Jin et al. (2020)	MMLU Hendrycks et al. (2021)
Domain	Clinical medicine (USMLE-style)	57 subjects (STEM, humanities, social sciences, etc)
Format	Vignette-style MCQs (single best)	4-option MCQ
Input	Clinical vignette text	Standalone question + 4 choices
Scale	Dev: 11,450; Test: 1,273	~15,908 total
Metric	Top-1 accuracy	Top-1 accuracy (few-shot)
Use	Clinical reasoning	General knowledge and reasoning

Table 2: Evaluation datasets for benchmarking biomedical and clinical knowledge in LLMs. Core benchmarks are listed alongside the MMLU medical subsets.

Category	Dataset	Size	Description
Core	MedQA (USMLE)	1,273	USMLE-style MCQs; clinical reasoning; general medical knowledge
MMLU	Clinical Knowledge	265	Applied clinical concepts (MCQs)
	Medical Genetics	100	Inheritance, molecular biology, disease associations
	Anatomy	135	Human anatomy and structural knowledge
	Professional Medicine	272	Advanced medical knowledge; professional practice
	College Biology	144	Undergraduate biology; medical foundations
	College Medicine	173	Pre-clinical medical knowledge; college-level curriculum

5.2 KNOWLEDGE GRAPH GENERATION RESULTS

We generated knowledge graphs (KGs) by extracting *Entity–Attribute–Value (EAV)* and *Entity–Relation–Entity (ERE)* triples from the *MMLU medical subsets* and *MedQA*. The pipeline used GPT-5, Gemini Flash 2.0, and Grok for gold-standard extraction, followed by QLoRA fine-tuning of LLaMA 3.1-8B. The fine-tuned extractor (rank $r=32$, $\alpha=16$, dropout 0.25; 1.36×10^7 trainable parameters, 0.30% of total) was trained for 20 epochs with AdamW, cosine decay, and dataset-specific learning rates (2×10^{-5} for MMLU, 2×10^{-4} for MedQA), producing reliable triples aggregated into structured KGs.

Table 3 shows cross-entropy training and validation losses: most MMLU subsets converge to low validation loss (≤ 0.7), while MedQA (0.97) is moderately higher, reflecting the complexity of USMLE-style vignettes. Table 4 summarizes structural statistics: MedQA yields the largest graph (36k triples; 22k nodes), with *Professional Medicine* the largest MMLU subset (11.7k triples) and *Medical Genetics* the smallest (2.4k triples). Across datasets, graphs are connected, moderately sparse, and well-suited for traversal and path-based reasoning.

Summary. The pipeline consistently produces large, connected, and moderately sparse KGs: MedQA and Professional Medicine yield tens of thousands of triples, while smaller subsets still form coherent graphs—providing a robust substrate for reasoning and explainable QA.

5.3 MMLU RESULTS

Figure 1 presents performance across **Accuracy**, **Precision (macro)**, **Recall (macro)**, and **F1 (macro)** on six MMLU medical subsets. Several observations emerge. First, *Medical Genetics* and *College Biology* show the strongest overall results, with all metrics exceeding 0.95, indicating both high correctness and balanced precision-recall performance. Second, *Anatomy (KG)* also achieves consistently high scores (~ 0.93), suggesting that structured knowledge grounding particularly benefits ontology-heavy domains. In contrast, *College Medicine* lags behind (~ 0.86 across metrics), reflecting greater complexity and variability in pre-clinical medical curricula. Finally, across all subsets, the closeness of accuracy, precision, recall, and F1 demonstrates that the model not only achieves high accuracy but also avoids bias toward particular answer classes, yielding stable performance under different evaluation perspectives. Together, these results confirm that **KG-QUEST** delivers robust, domain-aligned improvements across diverse medical reasoning tasks.

Table 5 summarizes representative accuracies on the original MMLU benchmark and its six medical subsets. On the overall benchmark, closed-source and open-source LLMs cluster in the mid-to-high

378
379
380 Table 3: Cross-entropy training and validation losses.
381
382
383
384
385
386
387

Dataset	Train Loss	Val. Loss
MMLU–Anatomy	0.43	0.51
MMLU–Clinical Knowledge	0.52	0.66
MMLU–Medical Genetics	0.57	0.63
MMLU–College Biology	0.61	0.78
MMLU–College Medicine	0.51	0.57
MMLU–Professional Medicine	0.68	0.70
MedQA	0.74	0.97

388
389 Table 4: Graph statistics of generated KGs.
390
391

Dataset / Subset	Triples	Entities	Attributes	Values	Nodes	Edges
MMLU–Anatomy	3,474	1,157	299	1,843	2,313	3,439
MMLU–Clinical Knowledge	5,399	1,845	442	2,921	3,690	5,399
MMLU–Medical Genetics	2,413	810	234	1,222	1,620	2,373
MMLU–College Biology	3,704	1,287	334	1,927	2,573	3,688
MMLU–College Medicine	4,839	1,650	458	2,519	3,301	4,839
MMLU–Professional Medicine	11,701	3,867	736	6,495	7,741	11,701
MedQA	35,955	11,065	2,067	19,800	22,142	35,955

399
400 80s: *GPT-4* reports 86.4% OpenAI (2023), *GPT-4o mini* reaches 82.0% Tong (2024), and *Llama-3*
401 70B achieves 88.6% Paul (2024). This saturation motivates evaluation on the medical subsets, which
402 remain more discriminative.

403 Across the six MMLU medical subsets, **KG-Quest (ours)** attains a macro average of **92.0%**,
404 outperforming the strongest prior average (90.5%) by nearly +1.5 points. KG-Quest sets new
405 state of the art on three subsets—*Anatomy* (+8.1 points), *Medical Genetics* (+1.0), and *College*
406 *Medicine* (+2.9)—and is competitive on the remaining three. Relative to GPT-4 (5-shot), KG-Quest
407 is higher on 5/6 subsets, with especially large gains in structure-heavy domains such as *Anatomy* and
408 *Medical Genetics*. These results demonstrate that *explicit KG grounding combined with sequence*
409 *modeling* improves reasoning fidelity beyond prompt-only large language models.

410 Table 5: Accuracies (%) on MMLU medical subsets. **KG-Quest (Ours)** compared against prior
411 baselines: GPT-4 and GPT-4-base (5-shot) OpenAI (2023), Med-PaLM 2 best and ER variants Nori
412 et al. (2024), and Flan-PaLM Nori et al. (2024). Bold indicates the best per row.

Dataset	KG-Quest (Ours)	GPT-4 (5-shot)	GPT-4-base (5-shot)	Med-PaLM 2 (best)	Med-PaLM 2 (ER)	Flan-PaLM (best)
Clinical Knowledge	87.9	86.4	88.7	88.7	88.7	80.4
Medical Genetics	98.0	92.0	97.0	92.0	92.0	75.0
Anatomy	93.3	80.0	85.2	84.4	84.4	63.7
Professional Medicine	91.0	93.8	93.8	95.2	92.3	83.8
College Biology	95.8	95.1	97.2	95.8	95.8	88.9
College Medicine	86.1	76.9	80.9	83.2	83.2	76.3
MMLU Average	92.0	87.4	90.5	89.9	89.4	78.0

423 424 5.4 MEDQA RESULTS 425

426 Table 6 presents representative results on MedQA (USMLE), alongside prior state-of-the-art and
427 baselines. Results are sorted from lowest to highest accuracy. Several trends emerge. First, early
428 baselines underperform: *Flan-PaLM (best)* achieves only 67.6%, while *GPT-4 (5-shot)* improves to
429 81.4%. Second, domain adaptation and explicit reasoning push performance higher: *Med-PaLM 2*
430 (*ER*) reaches 85.4%, and *Med-PaLM 2 (best)* slightly improves to **86.5%**, just above *GPT-4-base*
431 (*5-shot*) at 86.1%. Third, agent-based augmentation remains less effective: AGENTCLINIC records
56.1%, far below tuned LLMs.

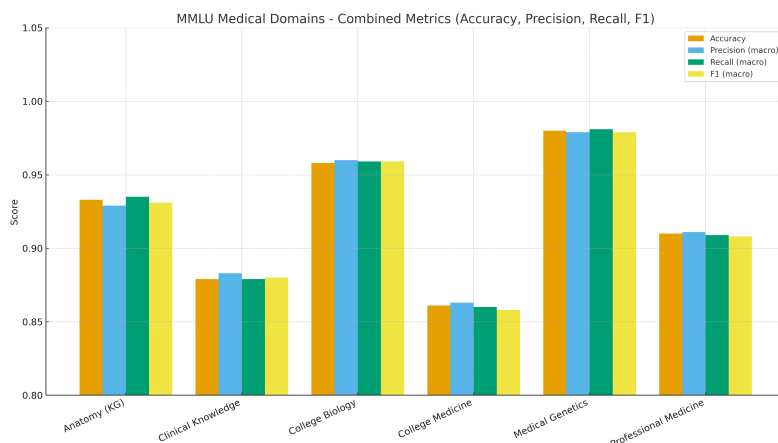


Figure 1: Performance on **MMLU medical domains** across combined metrics. Bars show Accuracy, Precision (macro), Recall (macro), and F1 (macro) for six subsets: Anatomy, Clinical Knowledge, College Biology, College Medicine, Medical Genetics, and Professional Medicine. The results highlight that KG-QUEST achieves consistent improvements across multiple evaluation criteria.

KG-QUEST (ours) delivers a substantial advance with a new state-of-the-art: macro accuracy of **93.7%**, macro F1 of **93.7**, and balanced per-class performance. In particular, KG-QUEST maintains high recall across all answer classes (ranging from 0.925 to 0.949), with the strongest performance on option D (F1 = 0.953). This demonstrates that explicit KG grounding not only improves overall accuracy but also reduces class-level variance compared to baselines.

Table 6: Representative results on **MedQA (USMLE)** benchmark, sorted from lowest to highest accuracy. **KG-QUEST (Ours)** achieves the strongest performance with macro metrics reported.

Model / Method	Accuracy (%)	Notes
KG-SFT Chen et al. (2025)	41.8	3-hop commonsense
AGENTCLINIC (Schmidgall et al., 2024)	56.1	agent tools (Notebook memory)
Flan-PaLM (best) Nori et al. (2024)	67.6	early generation baseline
GPT-4 (5-shot) OpenAI (2023)	81.4	general-purpose baseline
Med-PaLM 2 (ER) Nori et al. (2024)	85.4	explicit reasoning variant
GPT-4-base (5-shot) Nori et al. (2024)	86.1	reference setting
Med-PaLM 2 (best) Nori et al. (2024)	86.5	domain-tuned, instruction-optimized
KG-QUEST (Ours)	93.7	Macro: Prec.=93.7, Rec.=93.8, F1=93.7

Summary. KG-QUEST establishes a new SOTA on MedQA with **93.7%** macro accuracy and balanced per-class precision/recall, substantially outperforming Med-PaLM 2 and GPT-4 baselines. This highlights the effectiveness of KG-grounded reasoning in complex clinical QA tasks.

6 CONCLUSION

We introduced *KG-QUEST*, a framework that extends LLM-based QA with dynamically constructed, answer-specific knowledge graphs over EAV/ERE triples. By grounding inference in structured relations rather than static retrieval or parametric memory, KG-QUEST establishes new state-of-the-art performance: **92.0%** average accuracy on MMLU medical subsets and **93.7%** on MedQA (USMLE), substantially outperforming GPT-4 and Med-PaLM 2 baselines. These gains are especially pronounced in ontology-heavy domains such as Anatomy and Medical Genetics, where explicit KG grounding reduces hallucination and improves interpretability. Beyond accuracy, the pipeline produces large, connected, domain-consistent graphs that support transparent reasoning and robust error analysis. Looking forward, we will extend KG-QUEST to multimodal signals, long-context agentic retrieval, and real-world clinical decision support tasks beyond exam-style QA.

486
487
ETHICS STATEMENT488
489
490
491
492
493
494
495
We adhered to the ICLR Code of Ethics. This work uses only publicly available datasets (MMLU,
MedQA) that contain no personally identifiable information and are licensed for research use.
Potential risks include over-reliance on automated clinical decision support; to mitigate this, our
framework incorporates abstention and explicit evidence chains for interpretability. Fairness is
considered through macro metrics across answer classes, though no demographic attributes are
present in the datasets. No human subjects or patient data were collected, so IRB approval was not
required. We declare no conflicts of interest or external sponsorship that could influence this work.496
497
REPRODUCIBILITY STATEMENT498
499
500
501
502
503
We provide anonymized code and experiment scripts in the supplementary materials, including
dataset preprocessing, model configurations, and training schedules. Data splits, architectures,
hyperparameters, and extended ablation results are fully documented in the supplementary to ensure
transparency. All experiments were run with fixed random seeds, and environment files are included
to replicate the reported results. If the paper is accepted, we will release the full codebase and data
processing pipelines on GitHub to support community use and further research.504
505
LLM USAGE STATEMENT506
507
508
509
510
511
512
Large language models (LLMs), specifically OpenAI’s ChatGPT, were used to assist in paper
preparation. Their role was limited to language refinement, LaTeX formatting, and generating
alternative phrasings of author-written content. All scientific ideas, experimental design, analysis,
and claims were conceived, implemented, and verified by the authors. LLM outputs were carefully
reviewed and edited for accuracy. No part of the research methodology, data analysis, or results relies
on unverifiable LLM generation. The authors take full responsibility for the content of this paper.513
514
515
516
517
518
519
520
521
522
523
524
525
526
527
528
529
530
531
532
533
534
535
536
537
538
539

540 REFERENCES

542 Joshua Achiam et al. Gpt-4 technical report. *arXiv preprint arXiv:2303.08774*, 2023.

543 Akari Asai, Zeqiu Wu, Yizhong Wang, Avirup Sil, and Hannaneh Hajishirzi. Self-rag: Learning to
544 retrieve, generate, and critique through self-reflection. In *Proceedings of the Twelfth International*
545 *Conference on Learning Representations (ICLR)*, 2024.

546 Olivier Bodenreider. The unified medical language system (umls): integrating biomedical terminology.
547 *Nucleic acids research*, 32(suppl_1):D267–D270, 2004.

549 Antoine Bordes, Nicolas Usunier, Alberto Garcia-Duran, Jason Weston, and Oksana Yakhnenko.
550 Translating embeddings for modeling multi-relational data. In *Advances in Neural Information*
551 *Processing Systems*, 2013.

553 Kathi Canese and Sarah Weis. Pubmed: The bibliographic database. In *The NCBI Handbook*.
554 National Center for Biotechnology Information (US), Bethesda, MD, 2nd edition, 2013. URL
555 <https://www.ncbi.nlm.nih.gov/books/NBK153385/>.

556 Hanzhu Chen, Xu Shen, Jie Wang, Zehao Wang, Qitan Lv, Junjie He, Rong Wu, Feng Wu, and
557 Jieping Ye. Knowledge graph finetuning enhances knowledge manipulation in large language
558 models. In *The Thirteenth International Conference on Learning Representations*, 2025.

560 Aakanksha Chowdhery et al. Palm: Scaling language modeling with pathways. *Journal of Machine*
561 *Learning Research*, 24:1–113, 2023.

562 Darren Edge, Ha Trinh, Newman Cheng, Joshua Bradley, Alex Chao, Apurva Mody, Steven Truitt,
563 Dasha Metropolitansky, Robert Osazuwa Ness, and Jonathan Larson. From local to global: A
564 graph rag approach to query-focused summarization. *arXiv preprint arXiv:2404.16130*, 2024.

566 Dan Hendrycks, Collin Burns, Steven Basart, Andy Zou, Mantas Mazeika, Dawn Song, and Jacob
567 Steinhardt. Measuring massive multitask language understanding. In *International Conference on*
568 *Learning Representations*, 2020.

569 Dan Hendrycks, Collin Burns, Steven Basart, Andy Zou, Mantas Mazeika, Dawn Song, and
570 Jacob Steinhardt. Measuring massive multitask language understanding. *arXiv preprint*
571 *arXiv:2009.03300*, 2021. URL <https://arxiv.org/abs/2009.03300>. NeurIPS 2021
572 Datasets and Benchmarks Track.

574 Pengcheng Jiang, Cao Xiao, Minhao Jiang, Parminder Bhatia, Taha Kass-Hout, Jimeng Sun, and
575 Jiawei Han. Reasoning-enhanced healthcare predictions with knowledge graph community retrieval.
576 In *Proceedings of the Thirteenth International Conference on Learning Representations (ICLR)*,
577 2025.

578 Di Jin, Eileen Pan, Nassim Oufattolle, Wei-Hung Weng, Hanyi Fang, and Peter Szolovits. What disease
579 does this patient have? a large-scale open-domain question answering dataset from medical exams.
580 *arXiv preprint arXiv:2009.13081*, 2020. URL <https://arxiv.org/abs/2009.13081>.

581 Di Jin, Eileen Pan, Nassim Oufattolle, Wei-Hung Weng, Hanyi Fang, and Peter Szolovits. What
582 disease does this patient have? a large-scale open domain question answering dataset from medical
583 exams. *Applied Sciences*, 11(14):6421, 2021.

585 Qiao Jin, Bhuwan Dhingra, Zhengping Liu, William Cohen, and Xinghua Lu. Pubmedqa: A dataset
586 for biomedical research question answering. In *EMNLP-IJCNLP 2019*, pp. 2567–2577, 2019. doi:
587 10.18653/v1/D19-1259.

588 Alistair EW Johnson, Tom J Pollard, Lu Shen, Li-wei H Lehman, Mengling Feng, Mohammad
589 Ghassemi, Benjamin Moody, Peter Szolovits, Leo Anthony Celi, and Roger G Mark. Mimic-iii, a
590 freely accessible critical care database. *Scientific data*, 3(1):1–9, 2016.

592 Alistair EW Johnson, Lucas Bulgarelli, Lu Shen, Alvin Gayles, Ayad Shammout, Steven Horng,
593 Tom J Pollard, Sicheng Hao, Benjamin Moody, Brian Gow, et al. Mimic-iv, a freely accessible
electronic health record dataset. *Scientific data*, 10(1):1, 2023.

594 Xingxuan Li, Ruochen Zhao, Yew Ken Chia, Bosheng Ding, Shafiq Joty, Soujanya Poria, and Lidong
 595 Bing. Chain-of-knowledge: Grounding large language models via dynamic knowledge adapting
 596 over heterogeneous sources. In *The Twelfth International Conference on Learning Representations*,
 597 2024.

598 Shengjie Ma, Chengjin Xu, Xuhui Jiang, Muzhi Li, Huaren Qu, Cehao Yang, Jiaxin Mao, and Jian
 599 Guo. Think-on-graph 2.0: Deep and faithful large language model reasoning with knowledge-
 600 guided retrieval augmented generation. In *Proceedings of the Thirteenth International Conference*
 601 *on Learning Representations (ICLR)*, 2025.

602 Harsha Nori, Joshua M. Mayer, Nicholas King, Daniel Carignan, Eric Horvitz, Harlan M. Krumholz,
 603 and et al. Evaluation of med-palm 2 on medical question answering. *Nature Medicine*, 30:
 604 1032–1041, 2024. doi: 10.1038/s41591-024-03423-7.

605 OpenAI. Gpt-4 technical report. arXiv preprint arXiv:2303.08774, 2023. URL <https://arxiv.org/abs/2303.08774>.

606 Shirui Pan, Linhao Luo, Yufei Wang, Chen Chen, Jiapu Wang, and Xindong Wu. Unifying large
 607 language models and knowledge graphs: A roadmap. *IEEE Transactions on Knowledge and Data
 608 Engineering*, 2024.

609 Katie Paul. Meta releases newest ai model Llama 3 and ai assistant. *Reuters*, April 2024. News
 610 report.

611 Samuel Schmidgall, Rojin Ziae, Carl Harris, Eduardo Pontes Reis, Jeffrey Jopling, and Michael Moor.
 612 Agentclinic: a multimodal agent benchmark to evaluate ai in simulated clinical environments.
 613 *CoRR*, 2024.

614 Karan Singhal, Tao Tu, Juraj Gottweis, Rory Sayres, Ellery Wulczyn, Mohamed Amin, Le Hou,
 615 Kevin Clark, Stephen R. Pfohl, Heather Cole-Lewis, et al. Towards expert-level medical question
 616 answering with large language models. *Nature Medicine*, 2023a. Early online release prior to print,
 617 superseded by Singhal et al. (2025).

618 Karan Singhal, Tao Tu, Juraj Gottweis, Rory Sayres, Ellery Wulczyn, Mohamed Amin, Le Hou,
 619 Kevin Clark, Stephen R Pfohl, Heather Cole-Lewis, et al. Toward expert-level medical question
 620 answering with large language models. *Nature Medicine*, 31(3):943–950, 2025.

621 Karan Singhal et al. Large language models encode clinical knowledge. *Nature*, 620:172–180, 2023b.

622 Zhiqing Sun, Zhi-Hong Deng, Jian-Yun Nie, and Jian Tang. Rotate: Knowledge graph embedding by
 623 relational rotation in complex space. In *International Conference on Learning Representations*,
 624 2019.

625 Anna Tong. Openai unveils cheaper small ai model GPT-4o mini. *Reuters*, July 2024. News report.

626 Théo Trouillon, Johannes Welbl, Sebastian Riedel, Éric Gaussier, and Guillaume Bouchard. Complex
 627 embeddings for simple link prediction. In *International Conference on Machine Learning*, pp.
 628 2071–2080, 2016.

629 Bishan Yang, Wen-tau Yih, Xiaodong He, Jianfeng Gao, and Li Deng. Embedding entities and
 630 relations for learning and inference in knowledge bases. *arXiv preprint arXiv:1412.6575*, 2014.

631

632

633

634

635

636

637

638

639

640

641

642

643

644

645

646

647